ChemPubSoc Europe

DOI: 10.1002/chem.201406512

CHEMISTRY A European Journal Full Paper

Fluorescent Probes

Unravelling RNA–Substrate Interactions in a Ribozyme-Catalysed Reaction Using Fluorescent Turn-On Probes

Ece Cazibe Gaffarogullari,[a] Peter Greulich,[a] Andrei Yu. Kobitski,[b] Alexander Nierth,[a, c] G. Ulrich Nienhaus,[b, d, e, f] and Andres Jäschke*[a, f]

Abstract: The Diels–Alder reaction is one of the most important C–C bond-forming reactions in organic chemistry, and much effort has been devoted to controlling its enantio- and diastereoselectivity. The Diels–Alderase ribozyme (DAse) catalyses the reaction between anthracene dienes and maleimide dienophiles with multiple-turnover, stereoselectivity, and up to 1100-fold rate acceleration. Here, a new generation of anthracene-BODIPY-based fluorescent probes was developed to monitor catalysis by the DAse. The brightness of these probes increases up to 93-fold upon reaction with *N*-pentylmaleimide (NPM), making these useful tools for investigating the stereochemistry of the ribozyme-catalysed reaction. With these probes, we observed that the DAse catalyses the reaction with >91% *de* and >99% *ee*. The stereochemistry of the major product was determined unambiguously by rotating-frame nuclear Overhauser NMR spectroscopy (ROESY-NMR) and is in agreement with crystallographic structure information. The pronounced fluorescence change of the probes furthermore allowed a complete kinetic analysis, which revealed an ordered bi uni type reaction mechanism, with the dienophile binding first.

Introduction

RNAs perform various functions ranging from transmitting genetic information to regulation and catalysis. This functional diversity supports the RNA world hypothesis, in which DNA-protein based life evolved from an RNA-dominated pre-cellular soup.[1] The emergence of catalytically active RNAs (ribozymes) is believed to be among the first steps required for this transition.[1] An important aspect in the evolutionary theories is chirality, which is considered to be a key signature of life.[2]

Our research laboratories have a long-standing interest in ribozyme catalysis. A Diels–Alderase ribozyme (DAse) was selected by in vitro evolution and then rationally minimised.[3] The Diels–Alder reaction is central to organic chemistry and is frequently used for the assembly of ring systems. In the course of this reaction, up to four stereogenic centres are generated in a concerted manner. Although the relevance of enzyme-catalysed Diels–Alder reactions in natural biosynthetic pathways is still under debate,[4] several biopolymeric catalysts have been developed that accelerate the reaction and/or modulate its stereoselectivity.[5]

The DAse has been studied intensively over the years by applying a variety of experimental and computational techniques.[6] Nevertheless, very basic details, including the order of substrate binding or the molecular determinants of stereoselectivity, have not yet been experimentally validated.[6c,f] The combination of high K_M values, poor absorption and fluorescence properties of the Diels–Alder products, and low water solubility of substrates and products prevented comprehensive kinetic and mechanistic investigations.[6b,f] Recently, turn-on fluorescent dyads were developed in our laboratories to overcome these obstacles.[7] In these first-generation probes, the BODIPY fluorophore (4,4-difluoro-1,3,5,7-tetramethyl-4-bora-3a,4a-diaza-*s*-indacene) was attached to either C9 or C1 of the anthracene through a *meso*-phenyl ethynyl bridge (9-AB and 1-AB, Scheme 1). Anthracene was found to quench the BODIPY

[a] E. C. Gaffarogullari, Dr. P. Greulich, Dr. A. Nierth, Prof. Dr. A. Jäschke
Institute of Pharmacy and Molecular Biotechnology
Heidelberg University
Im Neuenheimer Feld 364, 69120 Heidelberg (Germany)
Fax: (+49) 6221-54-6430
E-mail: jaeschke@uni-hd.de

[b] Dr. A. Y. Kobitski, Prof. Dr. G. U. Nienhaus
Institute of Applied Physics, Karlsruhe Institute of Technology
Wolfgang-Gaede-Strasse 1, 76131 Karlsruhe (Germany)

[c] Dr. A. Nierth
Department of Chemistry, The Scripps Research Institute
10550 N. Torrey Pines Road, La Jolla, CA 92037 (United States)

[d] Prof. Dr. G. U. Nienhaus
Institute of Toxicology and Genetics
Karlsruhe Institute of Technology
Wolfgang-Gaede-Strasse 1, 76131 Karlsruhe (Germany)

[e] Prof. Dr. G. U. Nienhaus
Department of Physics, University of Illinois at Urbana-Champaign
1110 West Green Street, Urbana, IL 61801 (United States)

[f] Prof. Dr. G. U. Nienhaus, Prof. Dr. A. Jäschke
HEiKA—Heidelberg Karlsruhe Research Partnership
Heidelberg University, Karlsruhe Institute of Technology
(Germany)

Supporting information for this article is available on the WWW under http://dx.doi.org/10.1002/chem.201406512. It contains supporting figures and tables, and details of the synthesis of 1-DAPB derivatives and precursors of the 1-AB derivatives, optical spectroscopy, kinetic experiments, stereoselectivity measurements, and NMR spectroscopy.

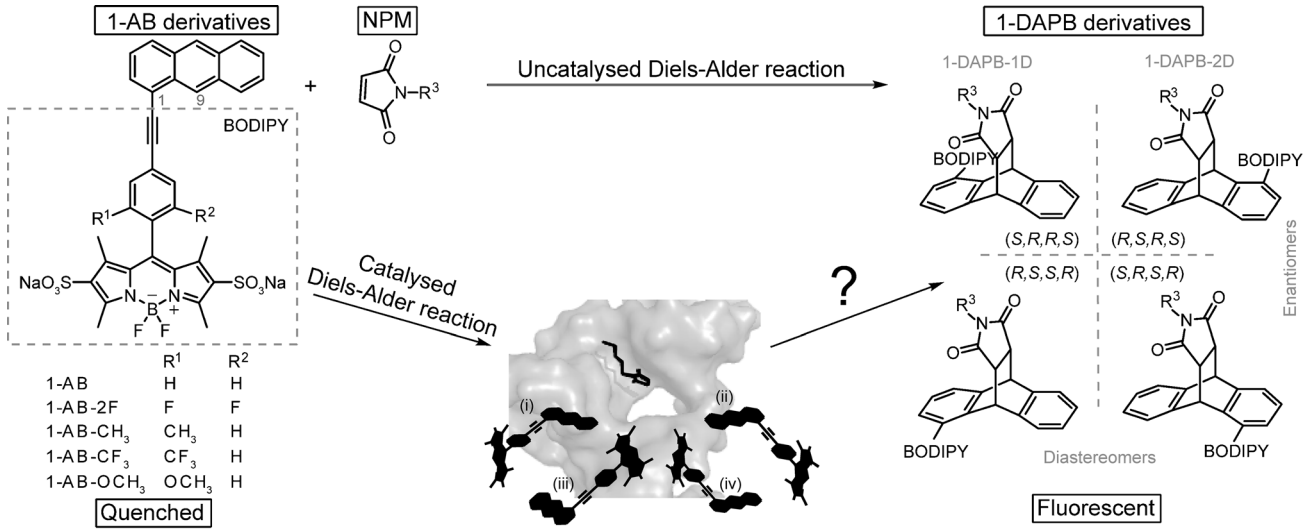

Scheme 1. The Diels–Alder reaction between 1-AB (1-anthracene–BODIPY) derivatives and NPM (*N*-pentylmaleimide, R^3: pentyl), creating four possible Diels–Alder-product-BODIPY (DAPB) stereoisomers. The 1-AB derivatives show only weak fluorescence, presumably due to a reductive photoinduced electron transfer (PET) from anthracene to BODIPY, whereas the DAPBs are highly fluorescent. To achieve four different DAPB, 1-AB derivatives may bind to the DAse in four different orientations: (i) head-first bulk-left; (ii) head-first bulk-right; (iii) tail-first bulk-left; (iv) tail-first bulk right. 3D structure of the DAse is adapted from PDB: 1YKV. In the 9-AB probe, the BODIPY group was attached through the 9-position of the anthracene as designated in the Scheme. The stereochemical designators of the 1-DAPB are explained in Figure S1 (see the Supporting Information).

fluorescence effectively, presumably by a reductive photoinduced electron transfer (PET) mechanism. Upon reaction with *N*-pentylmaleimide (NPM), a Diels–Alder-product-BODIPY (DAPB) conjugate was formed that was highly fluorescent due to disruption of the anthracene π-system. An up to approximately 20-fold increase in brightness upon Diels–Alder reaction could be achieved with the 1-AB and 9-AB probes, which allowed measurement of the reaction kinetics at high ribozyme concentration. However, for kinetic measurements under multiple-turnover conditions, the substrate concentrations should be much larger than the catalyst concentration. The 20-fold increase in brightness of the 1-AB and 9-AB probes was not sufficient to rise significantly above the background fluorescence generated by the unreacted probe. Therefore, probes with higher turn-on ratios were needed to fulfil the prerequisites of the kinetic analysis. 1-AB was a five-fold better substrate for the ribozyme than 9-AB, as judged by the rate of the catalysed reaction. Therefore, one aim of the current study was to improve the turn-on properties of the 1-AB probe by systematic chemical substitutions with electron-withdrawing or electron-donating groups (Scheme 1) to analyse the reaction kinetics of the DAse. A second aim was the application of these second-generation 1-AB probes for investigating molecular determinants of stereoselectivity. Previously, we probed the catalytic pocket with 9-substituted anthracenes and observed that increased steric bulk led to an increase in *ee* values of the Diels–Alder product. These findings supported the view that there is only limited space in the depth of the pocket ("behind" the bound substrate), forcing substituted anthracenes to bind preferentially in one specific orientation, namely "head-first" (head meaning the anthracene ring system).[5h,8] The new light-up probes based on a 1-substituted anthracene offer an additional degree of stereo-differentiation and allow ribozyme–substrate interactions to be probed at a new level of detail. In contrast to 9-substituted anthracenes, which, due to their symmetrical nature, can bind either head-first or tail-first, thereby creating product enantiomers, the asymmetrical 1-AB probes may bind in four different modes [i.e., head-first bulk-left (i), head-first bulk-right (ii), tail-first bulk-left (iii), tail-first bulk-right (iv); Scheme 1], leading to four stereoisomeric Diels–Alder products (two diastereomeric pairs of enantiomers). A quantitative analysis of the products formed in the ribozyme-catalysed reaction is therefore expected to provide new information on RNA–substrate interactions. On the basis of crystallographic data,[6a] we predicted that there is more space on the right-hand side of the DAse pocket, whereas there is more potential for collisions on the left-hand side (Scheme 1).

Herein we describe the design and synthesis of second-generation fluorescent turn-on probes based on the anthracene-BODIPY dyads. By using the probe with the highest light-up ratio, we revealed that the DAse efficiently synthesises only one of the four possible stereoisomeric products. The stereochemistry of this product was determined by ROESY-NMR analysis. The probe furthermore allowed sensitive kinetic analysis assuming rapid equilibrium conditions, revealing that the DAse follows an ordered bi uni reaction mechanism.

Results and Discussion

Design, synthesis and characterisation of the probes

We intended to improve the turn-on capabilities of the 1-AB probe by introducing different electron-withdrawing or electron-donating groups to the *meso*-phenyl ring *ortho* to BODIPY (depicted R^1 and R^2 in Scheme 1). The electronic effects of these substitutions are expected to change the highest occu-

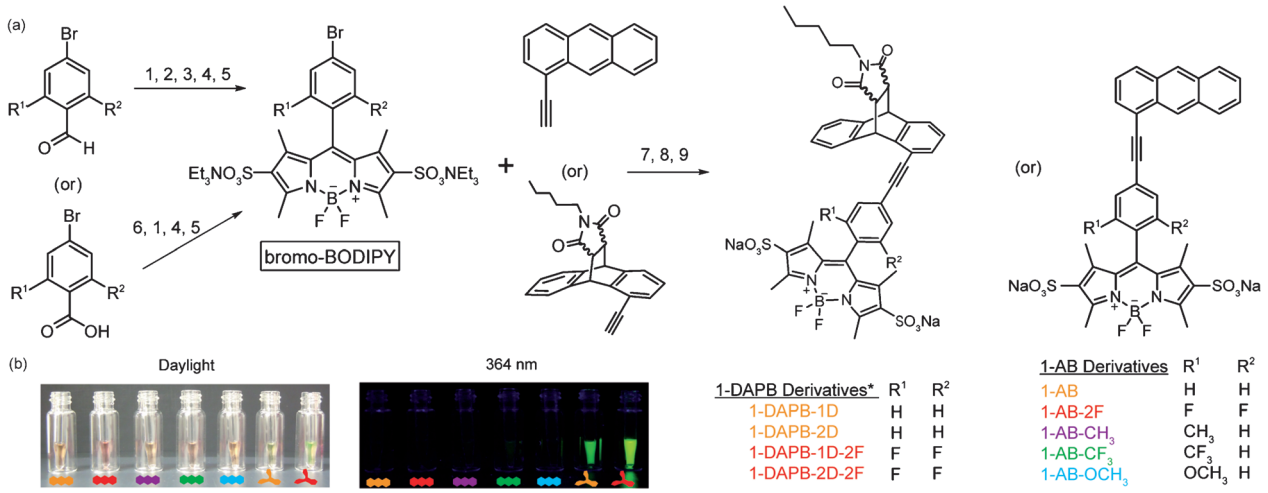

Scheme 2. Synthesis and characterisation of the BODIPY dyes a) Synthesis of 1-AB and 1-DAPB derivatives. Conditions: 1) pyrrole condensation; 2) acid catalysis; 3) oxidation; 4) BF_3 complexation; 5) sulfonation; 6) chlorination; 7) Sonogashira–Hagihara reaction; 8) ion exchange, and 9) further purification (see the Supporting Information for details). * Diastereomers for each of the 1D and 2D pairs. b) The daylight and 364 nm images of the BODIPY dyes synthesised by organic synthesis (100 μM dyes in water, 1-AB/1-DAPB, orange; 1-AB–2F/1-DAPB–2F, red; 1-AB–CH_3, purple; 1-AB–CF_3, green; 1-AB–OCH_3, blue).

pied/lowest unoccupied molecular orbital (HOMO/LUMO) energy levels, influencing the fluorescence intensity. Moreover, the *ortho* substitutions introduce further steric restrictions to the BODIPY systems,[9] which may prevent free rotation of the phenyl moiety with respect to BODIPY and influence dipolar relaxation pathways. We chose methyl, difluoro, methoxy, and trifluoromethyl substituents to cover both electronic and steric effects.

The new 1-AB-based probes, 1-AB–2F, 1-AB–CH_3, 1-AB–CF_3, and 1-AB–OCH_3, were synthesised in a similar manner to the first-generation probes by using a convergent route starting from commercially available benzaldehydes or benzoic acids (Scheme 2a; see the Supporting Information for experimental details).[7] Diels–Alder products of the probes were synthesised either by the ribozyme-catalysed reaction or by organic synthesis. Extensive purification ensured ultra-pure compounds with light-up properties (Scheme 2b, and Table S1 and Figure S2 in the Supporting Information). 1-DAPB diastereomers were separated by semi-preparative reverse-phase HPLC. The diastereomer with a lower retention time was named 1-DAPB-1D-R^1R^2 and the later-eluting isomer was named 1-DAPB-2D-R^1R^2 (see the Supporting Information, Figure S2).

All probes were tested for acceptance by the ribozyme under single-turnover conditions.[7] Reaction rates of all 1-AB type substrates were approximately five-fold higher than those reported for 9-AB (k_{cat}, 9-AB $= 2.5\times10^{-3}\,s^{-1}$),[7] and had similar rate constants (between 1.2×10^{-2} and $1.7\times10^{-2}\,s^{-1}$; Figure 1a and Figure S3 in the Supporting Information) with approximately 150-fold reaction rate acceleration. Thus, all 1-AB type substrates were better accepted by the DAse than 9-AB. Moreover, the chosen substitution positions had no detrimental effect on the RNA–substrate interactions. The increase in fluorescence of the probes upon Diels–Alder reaction, however, differed considerably, and 1-AB–2F was found to be the most efficient turn-on fluorophore (Figure 1b).

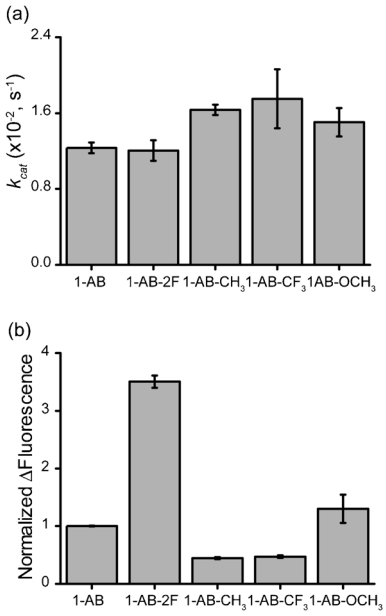

Figure 1. Selection of the best turn-on probe through a single-turnover kinetic experiment a) The apparent single-turnover rate constants (k_{cat}) of the 1-AB derivatives. Excess [DAse], 4.7 μM; and [NPM], 500 μM in standard DAse buffer were used over [1-AB derivatives], 0.13 μM to ensure a single-turnover. b) Selection of the best turn-on probe, 1-AB–2F, by single-turnover kinetic experiment. The increase in the fluorescence emission for the catalysed reactions was normalised with respect to 1-AB (see the Supporting Information, Figure S3 for the raw data). The error bars represent the range of the data ($n = 2$).

The spectroscopic analyses of the compounds are presented in Table 1, as well as Figures S4 and S5 in the Supporting Information. Variation of the *ortho* substituents at the *meso*-phenyl ring influenced the spectral properties and allowed fine-tuning of the absorption and emission maxima of the 1-AB derivatives (see the Supporting Information, Figure S6). In comparison to

Table 1. Spectroscopic properties of the 1-AB and 1-DAPB derivatives[a]

Compound	Absorption maxima (nm)		Fluorescence maxima [nm]		Quantum yield[b]
	Anthracene moiety	BODIPY moiety	Excitation	Emission	
1-AB	257, 311, 368, 386, 407;[b] 257, 314, 369, 386, 406[c]	500,[b] 501,[c,e] 504[d]	500,[b,c] 509[d]	511,[b] 512,[c,e] 524[d]	0.0078 ± 0.0002
1-AB–2F	258, 313, 372, 394, 413;[b] 257, 314, 373, 398, 419[c]	516,[b] 517,[c] 515[d]	511,[b,c] 520[d]	524,[b,c] 536[d]	0.0042 ± 0.0001
1-AB–CF_3	257, 312, 369, 388, 410;[b] 257, 312, 366, 389, 411[c]	507,[b] 508,[c] 511[d]	507,[b,c] 516[d]	516,[b,c] 530[d]	0.0168 ± 0.0006
1-AB–CH_3	257, 312, 368, 385, 406;[b] 257, 312, 366, 388, 408[c]	501,[b] 500,[c] 504[d]	500,[b,c] 510[d]	510,[b] 509,[c] 523[d]	0.0166 ± 0.0005
1-AB–OCH_3	257, 314, 369, 387, 407;[b] 257, 316, 369, 389, 409[c]	503,[b] 504,[c] 506[d]	502,[b] 503,[c] 512[d]	516,[b] 517,[c] 526[d]	0.0045 ± 0.0001
1-DAPB	n.a.	500,[b,f,g] 501,[c,f,g] 503[d,f,g]	501,[b,f,g] 503,[c,f,g] 510[d,f,g]	511,[b,f,g] 513,[c,f,g] 524[d,f,g]	0.109 ± 0.003,[f] 0.101 ± 0.002[g]
1-DAPB–2F	n.a.	514,[b,f,g] 515,[c,f,g] 515[d,f,g]	513,[b,f,g] 514,[c,f,g] 520[d,f,g]	524,[b,f,g] 525,[c,f,g] 536[d,f,g]	0.456 ± 0.014,[f] 0.379 ± 0.018[g]
1-DAPB–CF_3	n.a.	511[d,g]	516[d,g]	530[d,g]	n.d.
1-DAPB–CH_3	n.a.	504[d,g]	509[d,g]	523[d,g]	n.d.
1-DAPB–OCH_3	n.a.	506[d,g]	511[d,g]	526[d,g]	n.d.

[a] n.a. = not applicable, n.d. = not determined. Complete spectra of 1-AB and 1-DAPB derivatives can be found in Figures S4 and S5 in the Supporting Information, respectively. Raw data for quantum yield measurements are presented in Figure S7 in the Supporting Information. Fluorescence decay curves (see the Supporting Information, Figure S8), and fluorescence decay parameters (see the Supporting Information, Table S3) are given in the Supporting Information. [b] In water, [c] In standard DAse buffer, [d] In 55% (v/v) buffer A (0.1 M TEAA in H_2O, pH 7.4)/buffer B [0.1 M TEAA in MeCN/H_2O (8:2), pH 7.4], [e] ref. [7], [f] -1D, [g] -2D.

the unsubstituted 1-AB probe, 1-AB–CH_3 and 1-AB–OCH_3 had almost identical absorption, fluorescence excitation and emission spectra, whereas two fluorine-containing substrates, 1-AB–CF_3 and 1AB–2F, displayed a bathochromic shift. The Diels–Alder products of the corresponding anthracenes had absorption and emission maxima that were similar to those of the substrate molecules (Figure S6), which is consistent with the assumption of a PET-based quenching mechanism.[9b]

In all substrates, the BODIPY fluorescence is strongly quenched by anthracene. Quantum yields increase in the order 1-AB–2F < 1-AB–OCH_3 < 1-AB < 1-AB–CH_3 < 1-AB–CF_3 (Table 1 and Figure S7 in the Supporting Information). This trend could, however, not be directly correlated to steric or electronic substituent parameters (molecular volumes, Taft parameters, and Hammett coefficients),[10] suggesting a more complex combination of effects (data not shown). On the other hand, 1-DAPB–2F had a higher quantum yield and fluorescence lifetime compared with unsubstituted Diels–Alder BODIPY product, 1-DAPB (Table 1, and Table S3 and Figure S8 in the Supporting Information). This is in agreement with the observation reported by Kee et al. that substitutions on the *meso*-phenyl ring *ortho* to BODIPY cause a larger rotation angle of the phenyl ring with respect to the BODIPY plane.[11] This structural change suppresses the non-radiative decay channels, and causes a marked increase in fluorescence lifetime and quantum yield[11] (see the Supporting Information, Figure S8 and Table S3 for details).

As is evident from Table 1 and Figure 1b, 1-AB–2F had the lowest quantum yield and gave the highest increase in fluorescence amongst all 1-AB type substrates. 1-DAPB–2F/1-AB–2F had a brightness ratio of 93, which was approximately five times better than the 9-DAPB/9-AB[6c] or 1-DAPB/1-AB substrate/product couples (see the Supporting Information, Figure S9). Consequently, 1-AB–2F is the most suitable probe for further studies.

Stereoselectivity of the ribozyme-catalysed Diels–Alder reaction

To monitor the formation of the diastereomers in multiple-turnover experiments, the reactions were started by addition of NPM, stopped with β-mercaptoethanol, and analysed by reverse-phase HPLC with a fluorometric detector (Figure 2a). In the ribozyme-catalysed reaction, the formation of the 1-DAPB–2D-2F diastereomer was much faster than 1-DAPB–1D-2F, giving apparent pseudo-first-order rate constants of 5.6×10^{-3} and 0.1×10^{-3} s^{-1}, respectively, corresponding to selectivity (k_1/k_2) of 56. As seen in the HPLC traces (Figure 2b), almost all substrate was consumed after 120 min, and 1-DAPB–2D-2F was the major product of the DAse-catalysed Diels–Alder reaction with 92% *de*. The uncatalysed reaction was much slower, leaving 93% of the reactant even after 19 h, and only a slight diastereospecificity (17% *de*) was observed, independent of the time point (Figure 2b). A similar kinetic analysis performed on 1-AB yielded similar results (see the Supporting Information, Table S2 and Figure S10).

The different substitutions in the 1-AB turn-on probes may affect the dynamics of the BODIPY core with respect to the anthracene group, which, in turn, might have an effect on the selectivity in Diels–Alder reactions. Therefore, we measured the diastereoselectivity of the catalysed and uncatalysed reactions for all substrates (Table 2). Whereas the uncatalysed reactions showed only slight preferences (9 to 27% *de*), all ribozyme-catalysed reactions proceeded with high and similar diastereoselectivities of approximately 92 ± 1% *de*, indicating

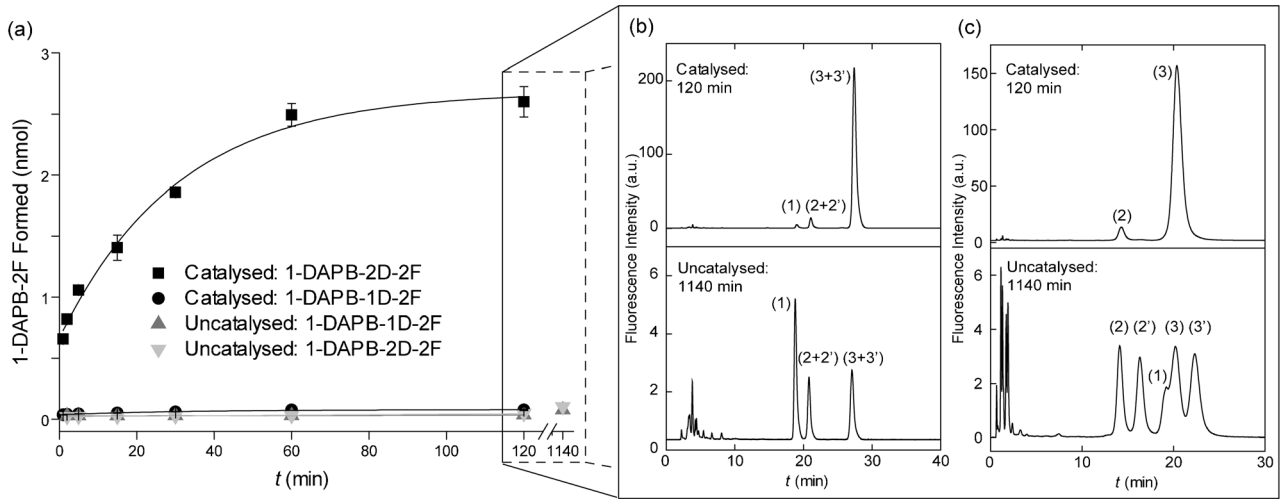

Figure 2. Analysis of the DAse stereoselectivity in multiple-turnover experiments by reverse-phase and chiral HPLC with a fluorescence detector a) Multiple-turnover kinetics of 1-AB–2F and NPM. Concentrations: [DAse], 7 μM; [1-AB–2F], 100 μM; and [NPM], 500 μM in standard DAse buffer at 24 °C. For the uncatalysed reaction, the DAse was omitted. The apparent rate constants are reported in Table S2 (see the Supporting Information). The error bars represent the standard deviation in $n=4$. b) The reverse-phase HPLC chromatogram (Ex: 475 nm, Em: 515 nm) and c) the chiral HPLC chromatogram (Ex: 505 nm, Em: 530 nm) of the catalysed and uncatalysed reactions after 120 min and 19 h, showing the diastereospecificity and enantiospecificity of DAse, respectively. (1) 1-AB–2F; (2) 1-DAPB–1D-2F (*R*,*S*,*S*,*R*); (2′) 1-DAPB–1D-2F (*S*,*R*,*R*,*S*); (3) 1-DAPB–2D-2F (*S*,*R*,*S*,*R*); (3′) 1-DAPB–2D-2F (*R*,*S*,*R*,*S*).

Table 2. Stereoselectivity of the Diels–Alder reaction[a]

Substrate	Uncatalysed		Catalysed	
	de	*ee*	*de*	*ee*
1-AB	27	<3	91	>99
1-AB–2F	17	<4	92	>99
1-AB–CF_3	26	n.d.	92	n.d.
1-AB–CH_3	27	n.d.	91	n.d.
1-AB–OCH_3	9	n.d.	93	n.d.

[a] n.d. = not determined.

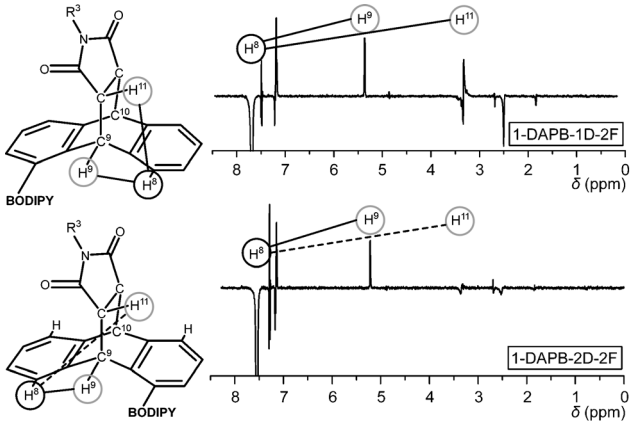

Figure 3. The 1D-ROESY-NMR spectra of 1-DAPB–1D-2F and 1-DAPB–2D-2F reveals the stereochemistry of the main product of the DAse catalysed reaction. The positive ROE interaction of the bridging hydrogen atoms (grey circles) to H-8 (black circle) of the anthracene are shown as solid lines. Dashed line indicates the absence of a ROE cross peak (R^3: pentyl).

that such intramolecular dynamics does not influence the stereochemical outcome in the catalysed reactions.

Previous experiments had established that 9-substituted anthracenes preferentially bind to the catalytic pocket in a "head-first" orientation (meaning that the unsubstituted long edge of the anthracene pointed into the pocket). Small and/or highly flexible substituents were, however, found to bind—to a lesser extent—in the "tail-first" orientation, making use of a small orifice in the back of the pocket, leading to *ee* values in the ribozyme-catalysed reaction between 16 and 90%.[5h, 6c, 8] On the basis of the ribozyme crystal structure and considering the rigidity and steric bulk of the BODIPY attached to anthracene, we presumed that such a "tail-first" binding is impossible for the 1-AB probes studied here. This hypothesis was tested by chiral HPLC analysis. For both 1-AB–2F (Figure 2c) and 1-AB (see the Supporting Information, Figure S11), only one enantiomer of each pair of diastereomers could be detected, resulting in >99% enantioselectivity, whereas racemic mixtures were obtained for the uncatalysed reactions (Table 2).

The stereochemistry of the main product 1-DAPB–2D-2F was assigned unambiguously by ROESY-NMR analysis of the chemically synthesised 1-DAPB–1D-2F and 1-DAPB–2D-2F reference compounds (Figure 3). The bridging hydrogen atoms, H-9 and H-11, are near to H-8 of anthracene in 1-DAPB–1D-2F, giving rise to positive ROE peaks between both H-8–H-9 and H-8–H-11. For 1-DAPB–2D-2F, however, H-8 is close in space to H-9, yielding positive ROE peaks, but very distant to H-11, giving no cross-relaxation peak.

Thus, by comparison with the HPLC traces of reaction products in the ribozyme-catalysed reaction, the main product was identified as the 1-DAPB–2D-2F (*S*,*R*,*S*,*R*) stereoisomer. This finding is in agreement with our prediction from crystallographic data,[6a] indicating that the steric demand of the BODIPY substituent not only prevents "tail-first" binding, but also "head-first, bulk-left", likely due to collisions with the RNA backbone,

enforcing mostly the head-first bulk-right binding, as shown in Scheme 1 (ii).

Binding order and kinetic scheme of the DAse-catalysed Diels–Alder reaction

The ribozyme-catalysed Diels–Alder reaction is a bi uni reaction, in which two reactants (bi) namely, a diene (1-AB–2F) and a dienophile (NPM) react to produce one product (uni), 1-DAPB–2F. Microscale thermophoresis experiments and molecular dynamics simulations suggested a positive cooperativity for substrate binding to the DAse and an ordered binding mechanism of the substrates, with NPM binding first, respectively.[6c,f] However, the exact binding order and kinetic scheme are still unknown, due to the poor solubility of the substrates and the lack of suitable methods for kinetic analysis. The 93-fold increase in 1-AB–2F brightness upon Diels–Alder reaction strongly enhanced the sensitivity of the detection of the reaction product, 1-DAPB–2D-2F, which, in turn, enabled us to use 14-fold lower concentrations of DAse compared with previous methods.[5h] This was crucial to meet the [DAse] $\ll$ [NPM] requirement for rapid equilibrium assumptions and allowed, for the first time, a complete kinetic analysis. Initial velocities at varying concentrations of both substrates were determined and analysed in double-reciprocal plots (Figure 4a and b). These plots are known to distinguish between an ordered and a random binding in two-substrate reactions (see the Supporting Information for the kinetic data treatment).[12] For the [NPM]-varied plots, the slope of the curves approached zero, and the reciprocal of apparent maximum velocities increased with rising 1-AB–2F concentration (Figure 4c). However, the double-reciprocal pattern for the [1-AB–2F]-varied plots looked different. The apparent maximum velocities were independent of NPM concentration and the slope of the curves did not approach zero (Figure 4d). Indeed, these kinetic data indicated an ordered reaction mechanism in which NPM binds first, then 1-AB–2F binds to the DAse/NPM complex (Figure 4e). Fitting of the experimental data to a rapid equilibrium ordered bi uni reaction mechanism (Equations SII-A and SII-B) gave Michaelis constants (K_M) of 566 $\pm$ 16 and 82 $\pm$ 7 μM for NPM and 1-AB–2F, respectively. The maximum velocity (V_{max}) was 8.5 $\pm$ 1 μM min^{-1}, which corresponds to a rate constant (k_p) of 17 $\pm$ 2 min^{-1}.

Conclusions

The Diels–Alder reaction is one of the cornerstones of organic chemistry. In this study, we investigated different aspects of catalyst–substrate interactions in a ribozyme-catalysed Diels–Alder reaction, namely the molecular determinants of stereoselectivity and the order of substrate binding. To overcome limitations from previous assays that were caused by an unfavourable combination of substrate/product solubility, detectability, and acceptance by the ribozyme, we designed and optimised a new class of molecular light-up probes that connect an anthracene diene with a substituted BODIPY dye. One of the probes, 1-AB–2F, which contains two fluoro-substituents at the *meso*-phenyl ring of BODIPY, was found to increase in brightness by approximately 93-fold upon Diels–Alder reaction, to be accepted as an excellent substrate by the ribozyme, and to show appreciable solubility in aqueous buffers. Therefore, 1-AB–2F finally allowed kinetic measurements at large excess of substrates over enzyme. By using this probe,

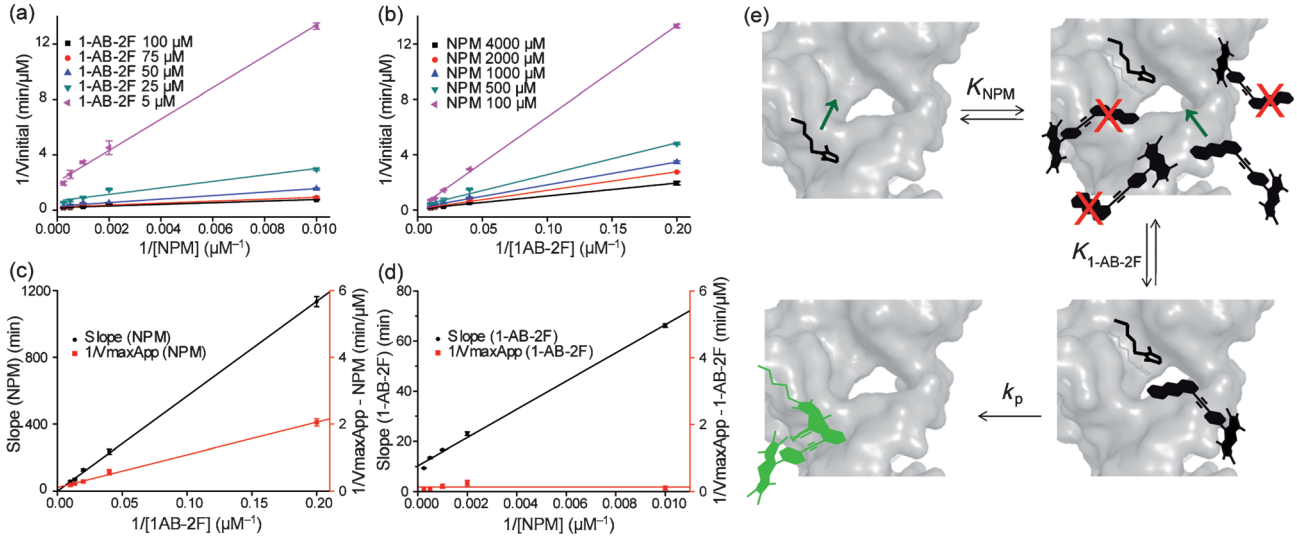

Figure 4. A complete kinetic analysis of the DAse and the proposed bi uni reaction mechanism. a) Lineweaver–Burk double reciprocal plot of the catalysed Diels–Alder reaction. [DAse]: 0.5 μM, [1-AB–2F]: 100 μM, black square; 75 μM, red circle; 50 μM, blue triangle; 25 μM, green triangle; and 5 μM, magenta triangle. b) Lineweaver–Burk double reciprocal plot of the catalysed Diels–Alder reaction. [DAse]: 0.5 μM, [NPM]: 4.0 mM, black square; 2.0 mM, red circle; 1.0 mM, blue triangle; 0.5 mM, green triangle; and 0.1 mM, magenta triangle (see the Supporting Information, Figure S12 for the raw data). c) Secondary re-plots of (a). d) Secondary re-plots of (b). For (c) and (d), $1/V_{maxApp}$ is the reciprocal of the apparent maximum velocity. In all plots, the error bars represent the standard deviation of triplicate measurements. e) The proposed reaction mechanism, in which NPM binds first, followed by 1-AB–2F binding with a specific orientation resulting in the formation of only one stereoisomer. Experimental data, (a)–(d), support an ordered bi uni reaction mechanism in which the Michaelis constants for NPM (K_{NPM}) and 1-AB–2F ($K_{1-AB-2F}$), and the rate constant (k_p) were fitted under rapid equilibrium assumptions.

we could establish that, with sterically demanding dienes such as 1-AB–2F, the ribozyme accelerates almost exclusively the formation of one of the four possible stereoisomers, namely 1-DAPB–2D-2F (*S*,*R*,*S*,*R*). Considering the crystallographic data and the highly dynamic nature of the ribozyme, this extraordinary selectivity is likely caused by the potential steric clashes between the diene and the ribozyme for different binding orientations.[6d,e,13] A second important finding of the current study that could only be obtained by using these light-up probes is that the DAse has an ordered bi uni reaction mechanism in which the dienophile binds first to the catalyst, followed by binding of the diene. A rate constant for the chemical step of approximately 17 min^{-1} was determined, in good agreement with earlier data,[5h] whereas the differences in the K_M values reflect both the different physical meaning of the constants depending of the mechanistic treatment (random bi uni vs. ordered bi uni) and the different chemical nature of the substrates used.

Although we developed the turn-on BODIPY probes to study the reaction mechanism of a ribozyme, they or their synthetic precursors might find applications in other fields. Preliminary data indicate that 1-AB derivatives are reactive (and light up) not only in Diels–Alder reactions with maleimides, but also in other cycloadditions, including those with reactive oxygen species. Furthermore, the bromo-BODIPY intermediates reported in Scheme 2a could be easily used for a one-step attachment to sensors or enzyme substrates other than anthracene to create light-up probes for a variety of analytes. Thereby, these compounds can address the limitations of BODIPY, especially with respect to biological systems, often caused by their poor water solubility.[9a,c]

Experimental Section

All solvents were purchased from Sigma–Aldrich and were used without further purification unless noted otherwise. Diels–Alderase ribozyme (DAse, 49-mer RNA sequence: 5′-GGA GCU CGC CCG GGC GAG GCC GUG CCA GCU CUU CGG AGC AAU ACU CGG C-3′ - synthesised on solid phase) was obtained from chemical synthesis services (CSS). Standard Diels–Alderase (DAse) buffer (300 mM NaCl, 30 mM Tris-HCl, 80 mM $MgCl_2$, 2 mM trolox, pH 7.4) was prepared as a 5× stock solution and diluted as required. DAse concentrations for the kinetic experiments were measured with a NanoDrop ND-1000 spectrophotometer (Peqlab Biotechnologie GmbH) by using the theoretical extinction coefficient of the DAse sequence, $\varepsilon_{260} = 453\,600\ M^{-1}\,cm^{-1}$. To ensure correct folding, a desired stock solution of DAse in water was refolded by heating for 2.0 min at 75 °C and controlled cooling in the thermoshaker (Eppendorf) within 20 min to RT.

1-AB derivatives were synthesised in a manner similar to that previously described by using appropriate bromo-BODIPY derivatives (1 equiv.), 1-ethynylanthracene (1.1 equiv.) and Sonogashira catalyst solution (see the Supporting Information for the preparation) in a microwave reactor (CEM2, Discover LabMate with a focused single-mode reaction chamber, 2.45 GHz).[7] The synthesised compounds were purified according to final purification and ion exchange steps (see the Supporting Information).

1-AB–2F: The reaction was set up with di-triethylammonium-2,6-disulfonate-1,3,5,7-tetramethyl-8-(4′-bromo-2′,6′-difluorophenyl)-4,4-difluoro-4-bora-3a,4a-diaza-*s*-indacene (100 mg, 125 μmol), 1-ethynylanthracene (28 mg, 138 μmol) and freshly prepared Sonogashira catalyst solution (3.0 mL). Yield: 71 mg (77 μmol, 62%); orange-red solid; $R_f = 0.20$ (buffer A/B, 1:1); ^{1}H NMR [500 MHz, CD_3OD/D_2O (5:2), 25 °C]: $\delta = 1.27$ (t, $J = 7.5$ Hz, 18H), 1.90 (s, 6H), 1.97 (s, 6H), 3.15 (q, $J = 7.5$ Hz, 12H), 7.44–7.52 (m, 5H), 7.77 (d, $J = 6.5$ Hz,1H), 8.01–8.02 (m, 2H), 8.06 (d, $J = 8.5$ Hz, 1H), 8.46 (s, 1H), 8.72 ppm (s, 1H); APT NMR [126 MHz, CD_3OD/D_2O (5:2), 25 °C]: $\delta =$ 9.26 (p), 9.85 (p), 11.59 (p), 12.45 (p), 15.80 (p), 47.77 (s), 92.27 (q), 92.81(q), 111.24 (q), 112.91 (q), 116.63 (t), 116.84 (t), 120.09 (q), 125.06 (t), 125.73 (t), 127.26 (t), 127.49 (t), 127.52 (t), 128.37 (t), 129.05 (t), 129.23 (q), 129.33 (q), 129.42 (q), 131.31 (q), 131.38 (t), 131.45 (q), 131.62 (t), 132.19 (q), 132.75 (q), 133.26 (q), 133.43 (q), 136.21 (q), 142.61 (q), 158.11 (q), 159.37 (q), 161.29 (q), 180.98 ppm (q); ^{19}F NMR [282 MHz, CD_3OD/D_2O (5:2), 25 °C]: $\delta = -143.50$ to −143.17 (m), −113.22 (s), −113.19 ppm (s); HRMS (ESI^-): *m/z* calcd for $C_{35}H_{23}BF_4N_2O_6S_2$ 359.0519 $[M]^{2-}$; found 359.0531.

1-AB–OCH_3: The reaction was set up with di-triethylammonium-2,6-disulfonate-1,3,5,7-tetramethyl-8-(4′-bromo-2′-methoxyphenyl)-4,4-difluoro-4-bora-3a,4a-diaza-*s*-indacene (50 mg, 63 μmol), 1-ethynylanthracene (14 mg, 69 μmol) and freshly prepared Sonogashira catalyst solution (2.0 mL). Yield: 31 mg (33 μmol, 53%); orange-red solid; $R_f = 0.15$ (buffer A/B, 1:1); ^{1}H NMR [500 MHz, CD_3OD/D_2O (5:2), 25 °C]: $\delta = 1.25$ (t, $J = 7.5$ Hz, 18H), 1.83 (s, 6H), 2.79 (s, 6H), 3.10 (q, $J = 7.5$ Hz, 12H), 3.88 (s, 3H), 7.14 (d, $J = 7.8$ Hz, 1H), 7.45–7.55 (m, 5H), 7.82 (dd, $J_1 = 7.8$ Hz, $J_2 = 0.6$ Hz, 1H) 8.03–8.12 (m, 3H), 8.52 (s, 1H), 8.89 ppm (s, 1H); APT NMR [126 MHz, CD_3OD/D_2O (5:2), 25 °C]: $\delta = 9.38$ (p), 9.88 (p), 11.66 (p), 13.02 (p), 15.88 (p), 47.76 (s), 56.85 (p), 89.89 (q), 94.76 (q), 115.50 (t), 121.10 (q), 124.81 (q), 125.29 (t), 125.88 (t), 126.51 (t), 127.21 (t), 127.42 (t), 127.61 (q), 128.27 (t), 129.06 (t), 129.31 (t), 130.70 (t), 130.92 (t), 131.55 (q), 131.74 (q), 131.99 (t), 132.39 (q), 133.27 (q), 133.40 (q), 135.34 (q), 143.21 (q), 143.41 (q), 156.33 (q), 157.70 ppm (q); ^{19}F NMR [282 MHz, CD_3OD/D_2O (5:2), 25 °C]: $\delta = -143.37$ to −143.13 ppm (m); HRMS (ESI^-): *m/z* calcd for $C_{36}H_{27}BF_2N_2O_7S_2$ 356.0666 $[M]^{2-}$; found 356.0704.

1-AB–CH_3: The reaction was set up with di-triethylammonium-2,6-disulfonate-1,3,5,7-tetramethyl-8-(4′-bromo-2′-methylphenyl)-4,4-difluoro-4-bora-3a,4a-diaza-*s*-indacene (50 mg, 64 μmol), 1-ethynylanthracene (14 mg, 69 μmol) and freshly prepared Sonogashira catalyst solution (2.0 mL). Yield: 32 mg (35 μmol, 55%); orange-red solid; $R_f = 0.15$ (buffer A/B, 1:1); ^{1}H NMR [500 MHz, CD_3OD/D_2O (5:2), 25 °C]: $\delta = 1.29$ (t, $J = 7.5$ Hz, 18H), 1.76 (s, 6H), 2.26 (s, 3H), 2.80 (s, 6H), 3.18 (q, $J = 7.5$ Hz, 12H), 7.31 (d, $J = 7.8$ Hz, 1H), 7.52–7.59 (m, 4H), 7.76–7.77 (m, 2H) 7.83 (d, $J = 7.0$ Hz, 1H), 8.09–8.16 (m, 3H), 8.57 (s, 1H), 8.93 ppm (s, 1H); APT NMR (126 MHz, CD_3OD/D_2O (5:2), 25 °C]: $\delta = 9.29$ (p), 11.60 (p), 12.97 (p), 14.60 (p), 15.82 (p), 19.19 (p), 47.84 (s), 88.40 (q), 93.53 (q), 119.96 (q), 123.47 (q), 124.05 (t), 124.68 (t), 124.80 (q), 125.98 (t), 126.19 (t), 126.98 (t), 126.99 (t), 127.81 (t), 128.10 (t), 128.25 (t), 129.57 (t), 129.62 (t), 130.31 (t), 130.54 (q), 130.62 (t), 131.17 (q), 132.03 (q), 132.17 (q), 133.23 (q), 134.16 (q), 134.51 (q), 135.03 (q), 136.23 (q), 142.21 (q), 155.66 (q), 170.50 (q), 175.29 (q), 175.97 ppm (q); ^{19}F NMR [282 MHz, CD_3OD/D_2O (5:2), 25 °C]: $\delta = -143.39$ to −143.06 ppm (m); HRMS (ESI^-): *m/z* calcd for $C_{36}H_{27}BF_2N_2O_6S_2$ 348.0691 $[M]^{2-}$; found 348.0720.

1-AB–CF_3: The reaction was set up with di-triethylammonium-2,6-disulfonate-1,3,5,7-tetramethyl-8-(4′-bromo-2′-trifluoromethylphenyl)-4,4-difluoro-4-bora-3a,4a-diaza-*s*-indacene (57 mg, 68 μmol), 1-ethynylanthracene (15 mg, 75 μmol) and freshly prepared Sonogashira catalyst solution (2.0 mL). Yield: 22 mg (23 μmol, 34%); orange-red solid; $R_f = 0.35$ (buffer A/B, 1:1); ^{1}H NMR {500 MHz, $[D_3]MeCN/D_2O$ (4:1), 25 °C]: $\delta = 1.20$ (t, $J = 7.5$ Hz, 18H), 1.71 (s, 6H),

2.78 (s, 6H), 3.01 (q, $J=7.5$ Hz, 12H), 7.54–7.60 (m, 4H), 7.68 (d, $J=7.0$ Hz, 1H) 7.91 (dd, $J_1=7.0$ Hz, $J_2=1.0$ Hz, 1H), 8.11–8.18 (m, 3H), 8.25–8.27 (m, 1H), 8.32 (d, $J=1.0$ Hz, 1H), 8.62 (s, 1H), 9.08 ppm (s, 1H); APT NMR {126 MHz, $[D_3]MeCN/D_2O$ (4:1), 25 °C}: $\delta=9.07$ (p), 11.31 (p), 13.00 (p), 14.60 (p), 15.59 (p), 47.45 (s), 91.34 (q), 93.19 (q), 120.41 (q), 121.77 (t), 125.41 (t), 125.85 (t), 126.35 (q), 127.21 (t), 127.33 (t), 128.24 (t), 128.89 (t), 129.35 (t), 129.35 (q), 131.07 (q), 131.10 (q), 131.17 (t), 131.33 (q), 131.98 (q), 132.13 (t), 132.39 (t), 132.88 (q), 132.90 (q), 133.12 (q), 133.14 (q), 133.17 (q), 136.26 (q), 136.27 (q), 137.25 (t), 140.98 (q), 142.43 (q), 156.94 ppm (q); ^{19}F NMR (282 MHz, $[D_3]MeCN$, 25 °C): $\delta=-143.84$ to -143.45 (m), -60.40 ppm (s); HRMS (ESI^-): *m/z* calcd for $C_{36}H_{24}BF_5N_2O_6S_2$ 375.0550 $[M]^{2-}$; found 375.0546.

Acknowledgements

We thank Tobias Timmermann for technical support. A. J. greatly acknowledges support by the Deutsche Forschungsgemeinschaft, SFB 623, BMBF, HEiKA, and the Helmholtz Initiative on Synthetic Biology. G.U.N. was funded by the KIT in the context of the Helmholtz STN program and HEiKA. E.C.G. was supported by a Landesgraduiertenförderung (LGFG) fellowship and the Hartmut Hoffmann-Berling international graduate school of molecular and cellular biology (HBIGS).

Keywords: cycloaddition · enantioselectivity · fluorescent probes · reaction mechanisms · ribozymes

[1] W. Gilbert, *Nature* **1986**, *319*, 618.
[2] D. G. Blackmond, *Cold Spring Harbor Perspect. Biol.* **2010**, *2*, a002147.
[3] B. Seelig, A. Jäschke, *Chem. Biol.* **1999**, *6*, 167–176.
[4] a) G. Pohnert, *ChemBioChem* **2001**, *2*, 873–875; b) H. Oikawa, T. Tokiwano, *Nat. Prod. Rep.* **2004**, *21*, 321–352; c) H. J. Kim, M. W. Ruszczycky, H. W. Liu, *Curr. Opin. Chem. Biol.* **2012**, *16*, 124–131.
[5] a) A. Togni, L. M. Venanzi, *Angew. Chem. Int. Ed. Engl.* **1994**, *33*, 497–526; *Angew. Chem.* **1994**, *106*, 517–547; b) C. E. Cannizzaro, J. A. Ashley, K. D. Janda, K. N. Houk, *J. Am. Chem. Soc.* **2003**, *125*, 2489–2506; c) J. M. Kang, J. Santamaria, G. Hilmersson, J. Rebek, *J. Am. Chem. Soc.* **1998**, *120*, 7389–7390; d) E. Alvira, C. Cativiela, J. I. Garcia, J. A. Mayoral, *Tetrahedron Lett.* **1995**, *36*, 2129–2132; e) A. C. Braisted, P. G. Schultz, *J. Am. Chem. Soc.* **1990**, *112*, 7430–7431; f) J. B. Siegel, A. Zanghellini, H. M. Lovick, G. Kiss, A. R. Lambert, J. L. St Clair, J. L. Gallaher, D. Hilvert, M. H. Gelb, B. L. Stoddard, K. N. Houk, F. E. Michael, D. Baker, *Science* **2010**, *329*, 309–313; g) M. Chandra, S. K. Silverman, *J. Am. Chem. Soc.* **2008**, *130*, 2936–2937; h) B. Seelig, S. Keiper, F. Stuhlmann, A. Jäschke, *Angew. Chem. Int. Ed.* **2000**, *39*, 4576–4579; *Angew. Chem.* **2000**, *112*, 4764–4768.
[6] a) A. Serganov, S. Keiper, L. Malinina, V. Tereshko, E. Skripkin, C. Hobartner, A. Polonskaia, A. T. Phan, R. Wombacher, R. Micura, Z. Dauter, A. Jäschke, D. J. Patel, *Nat. Struct. Mol. Biol.* **2005**, *12*, 218–224; b) F. Stuhlmann, A. Jäschke, *J. Am. Chem. Soc.* **2002**, *124*, 3238–3244; c) T. Berezniak, A. Jäschke, J. C. Smith, P. Imhof, *J. Comput. Chem.* **2012**, *33*, 1603–1614; d) T. Berezniak, M. Zahran, P. Imhof, A. Jäschke, J. C. Smith, *J. Am. Chem. Soc.* **2010**, *132*, 12587–12596; e) A. Y. Kobitski, A. Nierth, M. Helm, A. Jäschke, G. U. Nienhaus, *Nucleic Acids Res.* **2007**, *35*, 2047–2059; f) E. C. Gaffarogullari, A. Krause, J. Balbo, D. P. Herten, A. Jäschke, *RNA Biol.* **2013**, *10*, 1815–1821; g) N. Kisseleva, S. Kraut, A. Jäschke, O. Schiemann, *HFSP J.* **2007**, *1*, 127–136.
[7] A. Nierth, A. Y. Kobitski, G. U. Nienhaus, A. Jäschke, *J. Am. Chem. Soc.* **2010**, *132*, 2646–2654.
[8] R. Wombacher, S. Keiper, S. Suhm, A. Serganov, D. J. Patel, A. Jäschke, *Angew. Chem. Int. Ed.* **2006**, *45*, 2469–2472; *Angew. Chem.* **2006**, *118*, 2529–2533.
[9] a) A. Loudet, K. Burgess, *Chem. Rev.* **2007**, *107*, 4891–4932; b) N. Boens, V. Leen, W. Dehaen, *Chem. Soc. Rev.* **2012**, *41*, 1130–1172; c) G. Ulrich, R. Ziessel, A. Harriman, *Angew. Chem. Int. Ed.* **2008**, *47*, 1184–1201; *Angew. Chem.* **2008**, *120*, 1202–1219.
[10] a) A. Baldridge, S. R. Samanta, N. Jayaraj, V. Ramamurthy, L. M. Tolbert, *J. Am. Chem. Soc.* **2011**, *133*, 712–715; b) C. Hansch, A. Leo, R. W. Taft, *Chem. Rev.* **1991**, *91*, 165–195; c) R. W. Taft, *J. Am. Chem. Soc.* **1952**, *74*, 3120–3128; d) C. M. Timperley, W. E. White, *J. Fluorine Chem.* **2003**, *123*, 65–70.
[11] H. L. Kee, C. Kirmaier, L. H. Yu, P. Thamyongkit, W. J. Youngblood, M. E. Calder, L. Ramos, B. C. Noll, D. F. Bocian, W. R. Scheidt, R. R. Birge, J. S. Lindsey, D. Holten, *J. Phys. Chem. B* **2005**, *109*, 20433–20443.
[12] I. H. Segel, *Enzyme Kinetics: Behavior and Analysis of Rapid Equilibrium and Steady-State Enzyme Systems*, Wiley, Hoboken, **1993**.
[13] B. G. Keller, A. Kobitski, A. Jäschke, G. U. Nienhaus, F. Noe, *J. Am. Chem. Soc.* **2014**, *136*, 4534–4543.

Received: December 16, 2014
Published online on March 4, 2015